

Mechanism of the Asymmetric Sulfoxidation in the Esomeprazole Process: Effects of the Imidazole Backbone for the Enantioselection

Muthu Seenivasaperumal,^a Hans-Jürgen Federsel,^b and Kálmán J. Szabó^{a,*}

^a Stockholm University, Arrhenius Laboratory, Department of Organic Chemistry, SE 106 91 Stockholm, Sweden
Fax: (+46)-8-154908; e-mail: kalman@organ.su.se

^b Global Process R&D, AstraZeneca, SE 151 85 Södertälje, Sweden

Received: December 3, 2008; Revised: March 23, 2009

 Supporting information for this article is available on the WWW under <http://dx.doi.org/10.1002/adsc.200800753>.

Abstract: The asymmetric sulfoxidation reaction of imidazole-based prochiral sulfides was studied to explore the mechanistic details of the highly efficient esomeprazole process, which is one of the few industrial scale catalytic asymmetric procedures. The synthetic studies revealed that the smallest subunit governing the selectivity in the esomeprazole process is an imidazole ring. Thus, by using the esomeprazole procedure methyl imidazole sulfide could be oxidized as efficiently as its several functionalized derivatives, including pyrimetazol. However, alkylation of the imidazole nitrogen led to a major drop of the enantioselectivity. Our atmospheric pressure chemical ionization-mass spectrometry (APCI/MS) studies indicate that addition of small amounts of water to the reaction mixture facilitates the formation of mononuclear titanium species, which are the active catalytic intermediates of the selective oxidation reaction. One of the most important features of the esomeprazole procedure is that amine additives increase the enantioselectivity of the oxidation process. The NMR studies of the presumed reaction intermediates show that under catalytic conditions the amines are able to coordinate to titanium and disso-

ciate the coordinated imidazole substrate. The density functional theory (DFT) modelling studies provided new insights in the mechanism of the asymmetric induction. It was found that the oxidation requires a lower activation energy if the imidazole sulfide precursor does not coordinate to titanium. Two possible reaction paths were explored for this out of sphere oxidation mechanism. The most important interaction governing the enantioselection is hydrogen bonding between the N–H of the imidazole ring and the chiral tartrate ligand on titanium. Furthermore, the oxidation reaction imposes an important structural constraint to the TS structure involving a linear arrangement of the peroxide oxygens and the sulfur atom. This constraint and the N coordination of imidazole leads to a very strained structure for the inner sphere mechanism of the oxidation, which leads to a much higher activation barrier than the corresponding out of sphere process, and therefore it is unlikely.

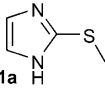
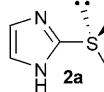
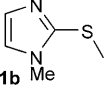
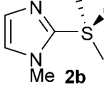
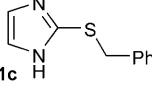
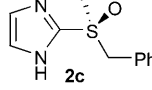
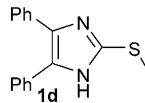
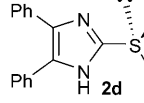
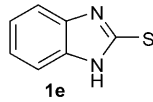
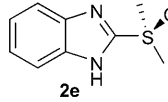
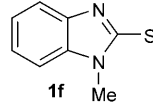
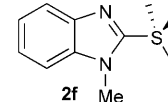
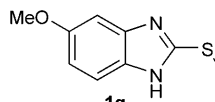
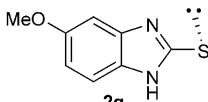
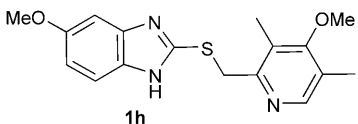
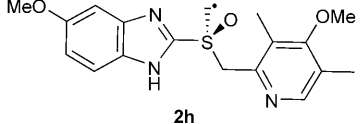
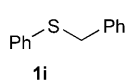
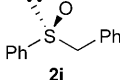
Keywords: asymmetric catalysis; density functional theory; nitrogen heterocycles; oxidation; sulfoxides; titanium

Introduction

Esomeprazole, the active ingredient of Nexium, is produced on a multi-ton scale per annum by using an efficient titanium tartrate-based asymmetric sulfoxidation process.^[1–3] This process is one of the few large-scale asymmetric catalytic applications that satisfies the rigorous selection criteria of atom economy and ecoefficiency required for modern industrial manufacturing processes.^[4] Accordingly, the esomeprazole

process has become an important source of inspiration and reference point for academic research to develop new efficient asymmetric catalytic methods relevant for the pharmaceutical industry and for the synthesis of specialized chemicals. Optically active sulfoxides,^[5–10] in general, represent an important class of pharmaceuticals and drug intermediates.^[11] They often play an important role as therapeutic agents, such as anti-ulcer (proton pump inhibitors),^[12–16] anti-bacterial, anti-atherosclerotic,^[17–19] anthelmintic,^[20]

Table 1. Dependence of the enantiomeric excess on the structure of the aromatic motif in asymmetric oxidation of prochiral sulfides.

Entry	Sulfide	Conditions ^[b]	Product	Yield [%] ^[c]	ee [%] ^[d]
1		-20/1.5		62	97
2 ^[e]	1a	-20/1.5	2a	57	92
3		35/2		33	<2
4		-20/1.5		61	95
5		-20/2		50	80
6		35/2		65	98
7		35/1		48	<2
8		-20/1.5		63	94
9		35/2		78	97
10		-20/1		64	10

^[a] The reactions were conducted in toluene according to the reaction conditions given in Figure 1.

^[b] Temperature/reaction time [°C/h].

^[c] Isolated yield.

^[d] Enantiomeric excess.

^[e] Chloroform was used as solvent.

sulfoxidation of **1a–h** is an imidazole ring with unsubstituted ring nitrogens. The high enantioselectivity is nicely maintained when the other substituent on the sulfur atom is a relatively bulky group such as in **1c** and **1h**. Considering these, we directed our further studies to the rationalization of the favourable features of the imidazole ring on the enantioselection in the titanium-catalyzed sulfoxidation reaction. Since **1a** and product **2a** are much easier to handle and much less bulky than pyrimetazole **1h** and esomeprazole **2h**, we employed these species as model compounds in our further experimental and modelling studies to ex-

plore the imidazole effects in the esomeprazole process.

Effects of the Added Water on the Outcome of the Catalytic Process

Addition of water to the titanium tartrate catalytic system is very important to achieve high levels of enantioselection in the sulfoxidation reaction.^[1,2,5,8,24] Kagan and co-workers pointed out that application of two equivalents of diethyl tartrate (**4**) relative to the

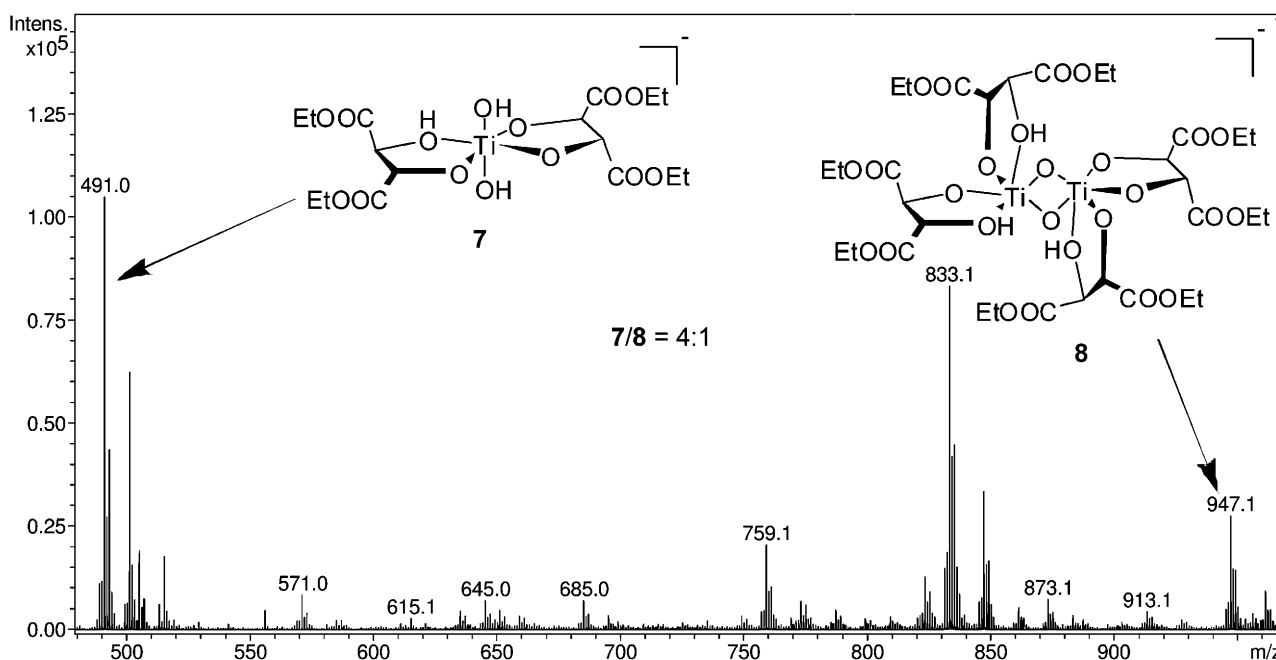


Figure 2. APCI mass spectrum of sample (i) prepared from **3** and **4** (1:2 ratio) in the absence of added water.

titanium catalyst **3** and application of water leads to a change of the structure of the Sharpless reagent^[52–54] generated when the **4** to **3** ratio is restricted to 1:1. The Sharpless reagent has a well-established binuclear structure,^[53,54] however, it is not *per se* efficient for the asymmetric sulfoxidation of prochiral sulfides.^[24] Consequently, the ratio of **3** to **4** and the amount of added water induce structural changes, which are specifically important for the asymmetric induction of the sulfoxidation reaction. In this respect the mechanistic picture given by Bolm and co-workers^[8] is particularly important. These authors assumed that the active species in the catalytic version of the sulfoxidation reaction (applying a 1:2 ratio for **3/4** and water as additive) is a monomeric titanium complex.

Mild ionization techniques^[55,56] based on atmospheric pressure chemical ionization (APCI) and electrospray ionization (ESI) have become useful tools for analysis of the reaction intermediates.^[57–59] Application of a mild ionization technique^[55,57] has also been indispensable in analysis of the intermediate complexes generated from **3**, **4** and water in the reaction conditions of the catalytic asymmetric oxidation of **1**. After extensive studies we have found that the APCI method (in negative ion mode) is more robust and efficient^[57] for the detection of the reaction intermediates, than the ESI method, and therefore this method was applied for the analysis of the reaction mixtures. In order to study the effects of added water, we have attempted to apply the reaction conditions of the equilibration step (see above) adapted to the ionization conditions of the APCI method. The choice of

the proper solvent is very important in this method to obtain mild but efficient ionization of the analyte. Unfortunately, toluene employed in the original procedure did not prove to be useful because of the inefficient ionization of the intermediate titanium complexes. This problem could be solved by replacement of toluene with chloroform, which proved to be a satisfactory medium for both the APCI analysis and for the enantioselective sulfoxidation reaction (Table 1, entry 2).

In order to explore the effects of the added water to the equilibration step of the sulfoxidation reaction, we have prepared two samples. The first sample (i) was prepared by dissolving diethyl tartrate **4** (2 equiv.) in 0.5 mL of chloroform at 50°C for 15 min followed by addition of titanium isopropoxide (**3**) (1 equiv.). This mixture was stirred at 50°C for further 45 min. The second sample (ii) was prepared in the same way, except that 1 µL water was also added. Prior to the APCI analysis, the samples were cooled down and diluted with 5 mL of chloroform. The dilution was required to obtain an optimal analyte concentration. The APCI analysis of sample (i) without added water showed two important peaks at $m/z = 491.0$ (**7**) and 947.16 (**8**) in a 4:1 ratio (Figure 2). We have found that addition of water induced significant changes in the spectrum. Thus, the APCI spectrum of sample (ii) showed that the ratio of the two species **7** and **8** was changed to 17:1.

Simulation of the isotope pattern (given in the supporting information) of the species at $m/z = 491.1$ indicated that this species (**7**) contains a single titanium

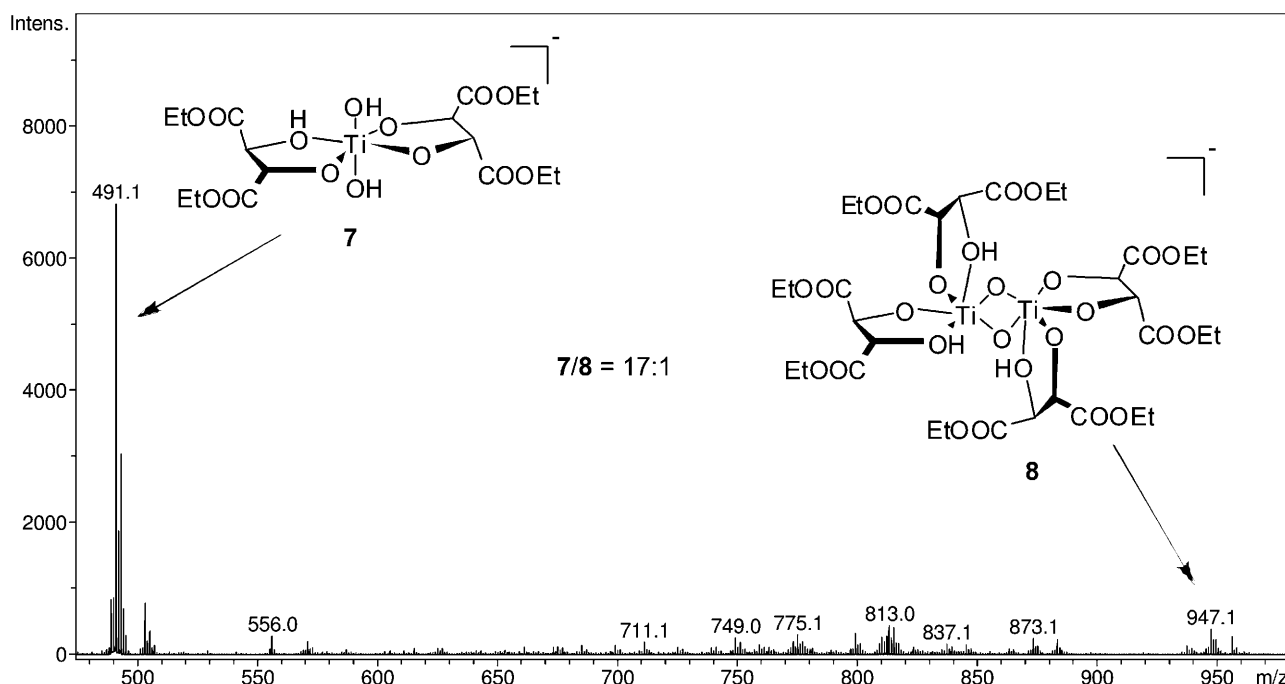


Figure 3. APCI mass spectrum of sample (ii) prepared from **3** and **4** (1:2 ratio) in the presence of added water.

atom, while the isotope pattern for the peak at $m/z = 947.1$ (**8**) is characteristic for a binuclear titanium complex. The MS/MS studies have shown that **7** and **8** are inter-related, as fragmentation of binuclear species **8** gave predominantly mononuclear species **7**. Considering the observed molecular weight of the complexes, our assumption is that **7** is a titanium di-tartrate complex, while **8** is a binuclear titanium complex incorporating four diethyl tartrate molecules (Figure 2 and Figure 3). The suggested hydroxy ligands may arise from water, which is certainly present in trace amounts even in sample (i) prepared without intentionally adding water.

Accordingly, addition of water increases the concentration of mononuclear species **7** at the expense of binuclear species **8** in the reaction mixture of the sulfoxidation. Furthermore, other intensive peaks (at $m/z = 833.1$ and 759.1 , Figure 2) generated by complexes with typically dinuclear isotope patterns are also suppressed or completely disappear in the presence of added water (Figure 3). These findings strongly suggest that the main role of the added water and also the use of excess of **4** is to generate a high concentration of monomeric titanium species, which are the active species of the catalytic process.^[8] Further

studies to establish the role of the substrate (**1**) and the applied amine (**5**) using APCI did not give unambiguous results, therefore we continued our studies with other techniques.

Role of the Amine Additive in the Sulfoxidation Process

Catalytic Studies

One of the most important differences between Kagan's^[24] Orsay procedure and the esomeprazole process^[1,2] is application of an amine base (such as **5a**) as a crucial component in the latter case. It was reported that the enantioselectivity of the oxidation of pyrmetazole (**1h**) to esomeprazole (**2h**) is lowered in the absence of Hünig's base (**5a**). Indeed, the selectivity of oxidation of **1a** to **1b** in the absence of **5a** shows a similar tendency (Figure 4). Thus, the enantioselectivity dropped from 97% (Table 1, entry 1) to 77%, when Hünig's base was not applied as additive.

It was shown that the esomeprazole process still works selectively by replacing **5a** with other amines.^[2] Likewise, we have found that replacement of **5a**

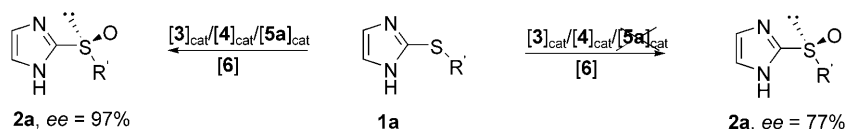


Figure 4. In the absence of **5a** the enantioselectivity of the sulfoxidation is decreased.

Table 2. Dependence of the selectivity on variation of the employed base.^[a]

Entry	Sulfide	Base	Product	Yield [%] ^[b]	ee [%]
1		(<i>i</i> -Pr) ₂ NEt 5a		62	97
2	1a		2a	65	98
3	1a		2a	46	89
4	1a		2a	52	82
5	1a		2a	48	88

^[a] The reactions were conducted at -20°C for 1.5 h in toluene according to the reaction conditions given in Figure 1.

^[b] Isolated yield.

(Table 2, entry 1) with imidazole (**5b**) or aniline derivatives **5c–e** affects only slightly the enantioselectivity. It is interesting to point out that imidazole **5b** (entry 2), which is the structural analogue of substrate **1a**, gives the same high selectivity as **5a**.

These findings show that the addition of amine additive increases the selectivity of the sulfoxidation, however Hünig's base can be replaced by several other species. In fact, substrate **1a** also incorporates a nitrogen atom, which may exert the same effects, as the corresponding functionality in **5a**. Considering the fact that imidazole (**5b**) could fully replace **5a** in the selective sulfoxidation reaction, it is reasonable to assume that *S*-methylimidazole **1a** is also able to act as nitrogen base in the process until it is consumed.

Indeed, we found that after 15 min of reaction time, when about 40% of substrate **1a** was still present in the reaction mixture (Table 3), the selectivity of the oxidation (94% *ee*) was about the same as in the presence of **5a** (97% *ee*, Table 1, entry 1). However, as **1a** was consumed, the *ee* was successively decreased to 77% until the conversion of **1a** was completed. Considering the fact that various nitrogen-containing species **5b–e** (Table 2) with different basicity are able to maintain the high selectivity of the sulfoxidation process, the main effect of **5a** in the enantioselection process is probably not exerted by a simple deprotonation of substrate **1a** but possibly *via* coordination to titanium. This would also explain the above observa-

Table 3. Selectivity in asymmetric oxidation of **1a** in the absence of **5a**.^[a]

Time [min] ^[b]	ee [%] ^[c]	Conversion of 1a [%] ^[d]
15	94	60
45	89	70
60	81	82
90	77	100

^[a] The reactions were conducted under standard condition in the absence of **5a** (Figure 6).

^[b] Elapsed reaction time.

^[c] Enantiomeric excess.

^[d] Conversion of **1a** determined by ^1H NMR.

tion that even without additives (such as **5a**) the enantioselectivity of the sulfoxidation of **1a** is high at low conversions (Table 3), as **1a** itself is available to coordinate to titanium, and thus enhance the enantioselectivity

Stoichiometric Studies to Detect Reaction Intermediates

The APCI/MS studies (see above) indicated that the conditioning process of the sulfoxidation reaction (see above) is very important to generate the active cata-

lytic intermediates of the reaction. Therefore, we have attempted to observe additional catalytic intermediates of the conditioning step. In these studies we mixed **1a**, **4** and water (1.0/0.3/0.15 equiv.) and heated them to 50°C for 15 min in chloroform followed by addition of **3** (0.15 equiv.), and heating at 50°C for 45 min. After this conditioning procedure, the reaction mixture was cooled and ether was added, which led to precipitation of a white solid. Unfortunately, we were not able to obtain crystals from this white solid, and therefore it was studied by NMR spectroscopy. The obtained substance was almost completely insoluble in chloroform, and therefore the NMR studies were carried out in MeOH-*d*₄. These studies have shown that the complex contained **1a** and diethyl tartrate **4** in a 1:1 stoichiometry. Considering the fact that the APCI studies indicated that the dominating species are mononuclear in the presence of water, we identified the white solid obtained in the conditioning process as a mononuclear titanium complex **9** (Figure 5, Table 4). Complexation of **1a** is also indicat-

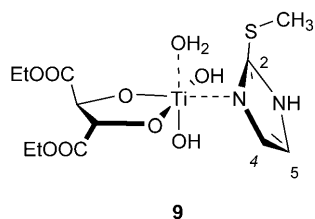


Figure 5. Tentative structure of the complex isolated from the reaction mixture of the conditioning process.

Table 4. Comparison of the NMR shift values of sulfide **1a** in **9** and in uncomplexed form.^[a]

Nucleus	Complex 9	Free 1a	Δ [ppm] ^[b]
H4, H5	7.34	7.04	0.30
SCH ₃	2.68	2.51	0.17
C4, C5	122.07	120.00	2.07
C2	142.25	140.62	1.63
SCH ₃	16.96	16.02	0.94

^[a] ¹H NMR (ppm) and ¹³C NMR (ppm) shift values recorded in MeOH-*d*₄.

^[b] Difference between the shift values of the complexed and free **1a**.

ed by the small but significant changes of the NMR shift values between its complexed and free forms (Table 4). Compound **1a** may coordinate *via* either its nitrogen or its sulfur atom to titanium. The N-coordination to titanium is suggested by the fact that the deviation of the ¹³C NMR shifts of **1a** is strongest for the double bonded carbons C4 and C5 (2.07 ppm), and still large for C2 (1.63 ppm), while it is relatively small for SCH₃ (0.94 ppm).

Subsequently, we have studied the behaviour of complex **9** on addition of Hünig's base **5a**. As mentioned above, complex **9** was practically insoluble in chloroform. However, when **5a** was added to a suspension of complex **9** the white solid was immediately dissolved indicating that amine **5a** is coordinated to the complex, which became readily soluble in chloroform. Coordination of **5a** to titanium could be confirmed by systematic changes of its NMR shifts (Figure 6, Table 5). In particular, the shift value of C1 and C2 changed (by 3.38 and 2.29 ppm) in **5a** after addition to complex **9** (Figure 6). On the other hand the shift values of substrate **1a** in this reaction mixture and in free form agreed within 0.5 ppm (Figure 6), and therefore we conclude that coordination of **5a** leads to dissociation of **1a** from complex **9**. Overall, addition of Hünig's base **5a** to complex **9** obtained from the reaction mixture of the conditioning process triggers a ligand exchange process, in which **5a** replaces **1a**.

We have also employed complex **9** as catalyst in the asymmetric oxidation of **1a** (Figure 7). These studies have shown that complex **9** is an active catalyst in the sulfoxidation. In the presence of **5a** product **2a** was afforded with a relatively good selectivity. When the re-

Table 5. Comparison of the ¹³C NMR shift values of **5a** in complex **10** and in its free form.^[a]

Carbon	Complex 10	Free 5a	Δ [ppm] ^[b]
C1	51.79	48.41	3.38
C2	41.28	38.99	2.29
C3	19.75	20.58	-0.83

^[a] Shift values recorded in CDCl₃. Numbering of **5a** is given in Figure 6.

^[b] Differences between the shift values of the complexed and free **5a**.

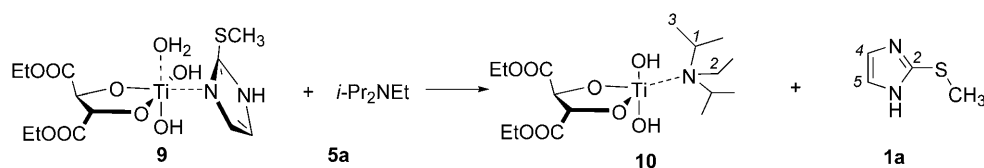


Figure 6. Addition of Hünig's base to **9** leads to formation of **10** by ligand exchange.

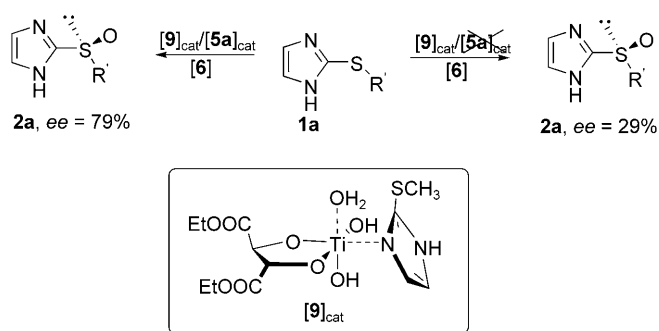


Figure 7. Application of complex **9** as catalyst in the sulfoxidation reaction in the presence and absence of **5a**.

action was carried out without amine **5a** the enantioselectivity was significantly lowered, similar to the original process carried out according to the esomeprazole procedure^[1,2] (Figure 4). The fact that complex **9** in the presence of **5a** shows a high catalytic activity and relatively good enantioselectivity indicates that **9** and **10** and/or closely related analogues are the true reaction intermediates of the sulfoxidation reaction of **1a** in the esomeprazole procedure.

The results presented in this section indicate that **5a** and other amines (Table 2) are important additives in the esomeprazole procedure to increase the enantioselectivity of the process. In the first conditioning step, a titanium-diethyl tartrate (DET) substrate complex (such as **9**) is formed, which then undergoes ligand exchange with the amine additive to give a new titanium-DET amine complex (such as **10**). Accordingly, **5a** (or other amines) serves as a ligand on titanium, and its ligand effects are important to increase the enantioselectivity of the sulfoxidation process.

The results of this and the previous sections give important suggestions about the active intermediates and give several hints for a rationalization of the mechanism leading to the enantioselection. Based on these results, the steric and electronic effects of the tartrate and the amine ligands (**4** and **5**, respectively) on the enantioselection process were studied by DFT modelling studies.

DFT Modelling Studies of the Mechanism of the Enantioselection

In spite of the large importance of titanium-catalyzed asymmetric sulfoxidation reactions, there are surprisingly few theoretical studies published on the mechanism of the oxidation and the possible ways of the chiral induction. Jørgensen^[60] has published a study on the mechanism of the sulfoxidation modelling the Orsay conditions.^[24] This work involved a quantum chemical (Hartree–Fock) study of the core reaction,

which was modelled by strongly simplified species, as, at the date of this study (1994) inclusion of the tartrate ligand, was not realistic. The possible mechanism of the enantioselection was studied by molecular mechanics calculations. In these studies Jørgensen^[60] also gave a useful MO interpretation for the transition state of the oxidation step, which nicely rationalizes the geometrical constraints imposed by the transfer of the oxygen atom from the titanium coordinated peroxide molecule to the sulfur atom of the pro-chiral sulfide.

Our main intention was, of course, the modelling of the enantioselection of the esomeprazole process by DFT calculations. As we have shown (see above) methylimidazole **1a** is oxidized as efficiently and selectively as pyrimetazole, we thus chose this species as the prochiral sulfide for the modelling studies. In fact, from the very beginning of the project we have intended to find the smallest possible prochiral sulfide substrate to decrease the computational burden of the modelling studies.

Computational Methods

All geometries were fully optimized employing a Becke-type^[61] three-parameter density functional model B3LYP^[62,63] using a 6-31G* basis set.^[64,65] Harmonic frequencies have been calculated at the level of optimization for all structures to characterize the calculated stationary points and to determine the zero-point energies and other thermodynamical energy contributions. Fully optimized transition state structures **11–13R/S-TS** (Figure 11, Figure 12, Figure 13) have been characterized by a single imaginary frequency, while the rest of the optimized structures possess only real frequencies. All calculations were carried out by employing the Gaussian 03 program package.^[66]

Modelling Strategies

The relatively small prochiral substrate allowed us to perform a DFT modelling study with only minor truncation of the realistic reaction components. The simplifications involved the following: (i) in the modelling studies we employed dimethyl tartrate, instead of diethyl tartrate; (ii) Hünig's base **5a** was replaced by trimethylamine; (iii) cumene peroxide was modelled by methyl peroxide; and (iv) the isopropoxide ligand was replaced by a methoxide ligand. Considering our findings on the effect of water (see above) and previously published mechanistic suggestions,^[8,60] we performed the DFT calculations for mononuclear complexes. The peroxide molecule was assumed to coordinate in an η^2 -fashion to the titanium atom in line with

previous studies and mechanistic suggestions,^[8,60,67]. Although, Kagan has pointed out that the sulfide substrate is probably not coordinated to titanium under the sulfoxidation reaction (and our studies^[51] have confirmed this suggestion), we studied two distinct oxidation pathways: (i) without coordination of imidazole sulfide (**1a**) to titanium (Figure 8 and Figure 9). In this case trimethylamine is coordinated to titanium (see above); and (ii) when **1a** is coordinated to titanium and undergoes an inner-sphere oxidation process (Figure 10).

The Out of Sphere Mechanism of the Sulfoxidation

We have localized (Figure 8 and Figure 9) two distinctly different Ti-tartrate-peroxide complexes with a coordinated Me_3N molecule (**11** and **12**). In these complexes **1a** is not able to directly coordinate to titanium (Figure 11 and Figure 12). However, **1a** is bound to the tartrate ligand by a firm hydrogen bonding. This hydrogen bond involves the N–H proton of the imidazole ring and the alkoxide (**11**, Figure 11) or the carbonyl group (**12**, Figure 12) of the tartrate ligand. This hydrogen bonding is very important in position-

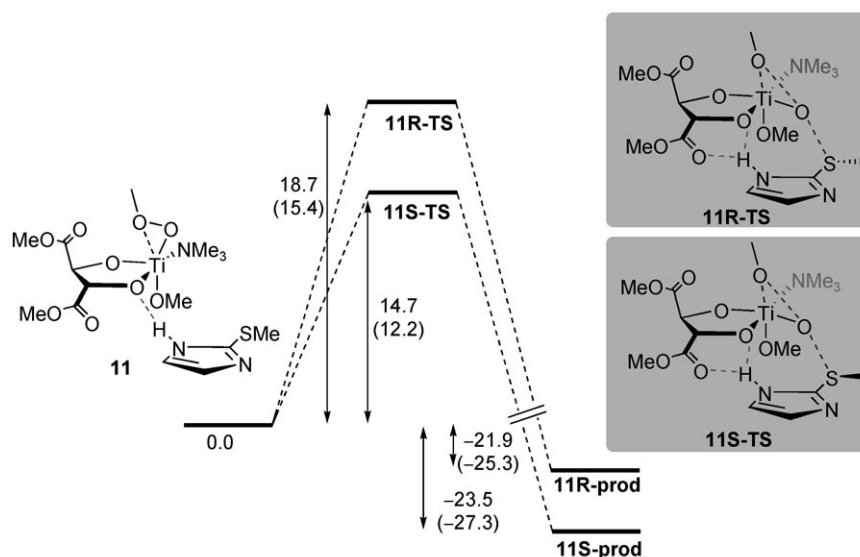


Figure 8. Reaction path Ia for out of sphere oxidation of methyl imidazole sulfide **1a**. The Gibbs free energy values and the total energy differences (in parentheses) are given in kcal mol^{-1} .

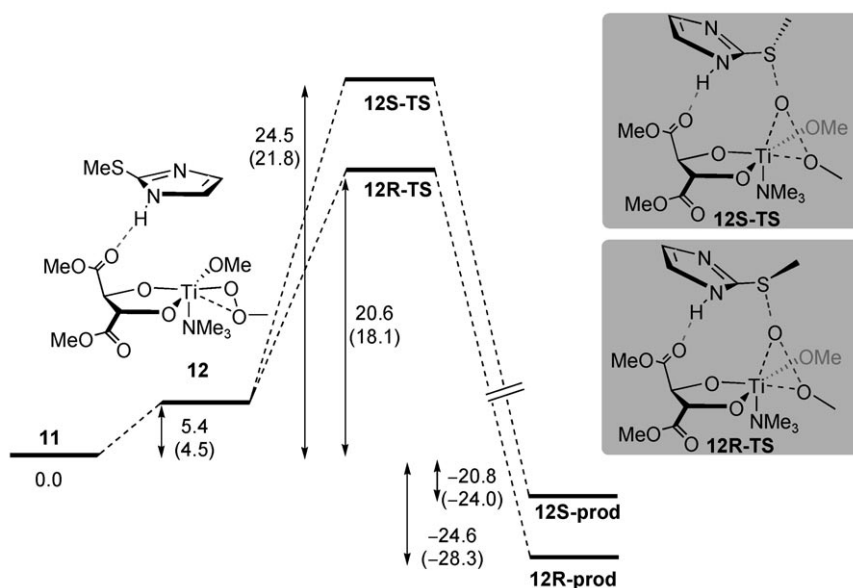


Figure 9. Reaction path Ib for out of sphere oxidation of methyl imidazole sulfide **1a**. The Gibbs free energy values and the total energy differences (in parentheses) are given in kcal mol^{-1} .

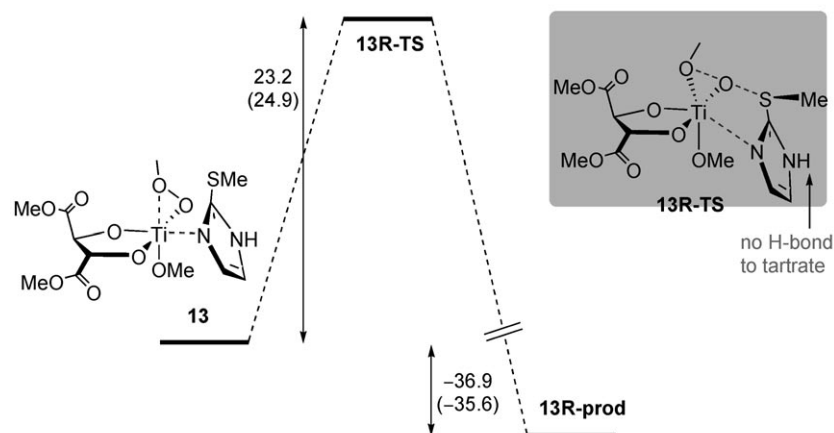


Figure 10. Reaction path II for inner sphere oxidation of methyl imidazole sulfide **1a**. The Gibbs free energy values and the total energy differences (in parentheses) are given in kcal mol⁻¹.

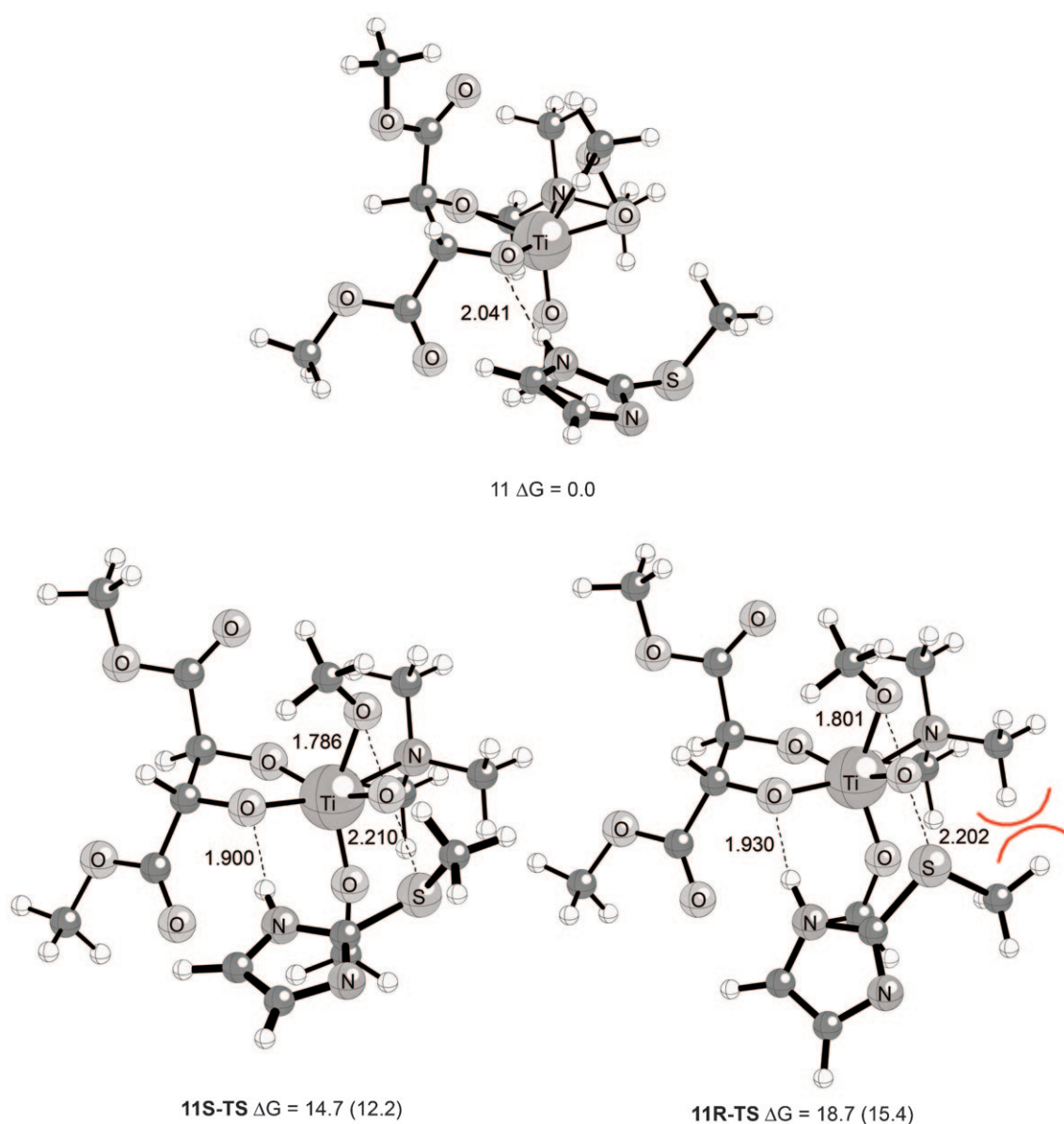


Figure 11. Selected calculated structures for path Ia (cf. Figure 8). The distances are given in Å units and the Gibbs free energy values and the total energy differences (in parentheses) are given in kcal mol⁻¹.

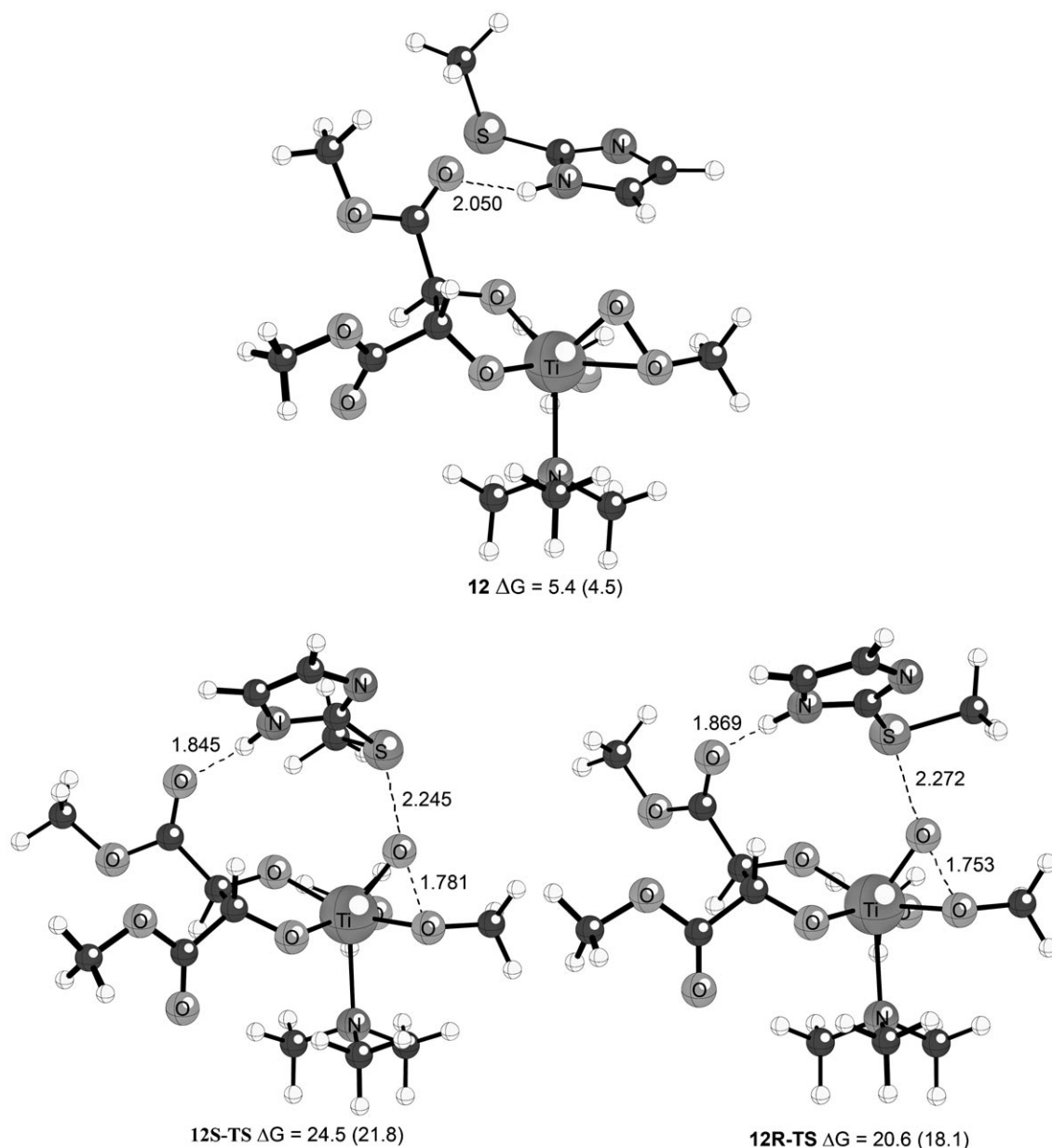


Figure 12. Selected calculated structures for path Ib (cf. Figure 9). The distances are given in Å units and the Gibbs free energy values and the total energy differences (in parentheses) are given in kcal mol⁻¹.

ing of the pro-chiral sulfide (**1a**) with respect to the chiral titanium complex, and it is also preserved under the entire oxidation process.

Path Ia: Complex **11** is more stable than **12** by 5.4 kcal mol⁻¹. In this complex (**11**) the N–H proton of the imidazole molecule is coordinated to the front side alkoxide atom of the tartrate ligand (Figure 11). The rear side of the tartrate molecule is effectively blocked by the Me₃N ligand. Two TS structures were localized for the oxidation reaction starting from complex **11**. TS structure **11S-TS** gives the *S*-form of the product (**2a**), while **11R-TS** leads to the *R* configured counterpart. Formation of the *S*-product (**11S-TS**) re-

quires a lower activation barrier by 4 kcal mol⁻¹ than the *R* form (**11R-TS**). Since formation of the *S*-product (**11S-prod**) of path Ia represents the lowest energy reaction path compared to other possible reaction channels (path Ib and path II), our theoretical model predicts predominant formation of methylimidazole sulfoxide with *S*-configuration (**2a**), which is in agreement with the experimental findings (Table 1).

One of the most important structural features of the TS structure (**11S-TS**) is the geometry of the reaction coordinate involving the oxygen atoms of the peroxide molecule and the sulfur atom of **1a** (Figure 11). The reaction coordinate indicates cleav-

age of the oxygen-oxygen bond (1.786 Å) with a simultaneous formation of the oxygen-sulfur bond (2.210 Å) involving one of the lone-pairs of the sulfur atom. The O–O–S angle is very close to 180° imposing a special geometrical constraint to the TS structure of the oxidation.^[68] The major difference in the structure of **11S-TS** and **11R-TS** is the conformation of the methyl group in the SMe functionality. The lower stability of **11R-TS** compared to **11S-TS** can be explained by the steric interaction between the methyl group of **1a** and Me₃N ligand in **11R-TS**. As this interaction is not present in **11S-TS** selective formation of the *S*-sulfoxide (**2a**) product takes place. The substrate position relative to the chiral tartrate ligand is determined by hydrogen bonding. Of course, in the absence of an N–H group in the imidazole ring such hydrogen bonding cannot exist. This may explain the low selectivity obtained for the oxidation of **1b** (Table 1, entry 3). On the other hand the possible substituents at the C4 and C5 of the imidazole ring as well as bulkier substituents on the sulfur are easily tolerated in **11S-TS**, since these positions are not involved in any major steric interaction with the ligands of the complex (Figure 11). This may explain the experimentally observed fact that in the presence of bulky substituents at the C4, C5 (e.g., **1d–e** and **1g–h**) and SR (**1c** and **1h**) positions the high enantioselectivity of the oxidation can be maintained (Table 1). The reactions are highly exothermic (by 20–25 kcal mol⁻¹), and thus (as expected) the sulfoxidation process is irreversible.

Path Ib: Reaction path Ib starts with complex **12**, which is less stable than complex **11** of path Ia. In complex **12** the substrate molecule (**1a**) is bound to the rear side of the tartrate molecule by hydrogen bonding. This mode of coordination in **12** renders **1a** to the opposite side of the complex compared to **11** suggesting different selectivity for paths Ia and Ib.

Indeed, in path Ib the *R*-product (**12R-prod**) is formed via a lower barrier (**12R-TS**) than the *S*-product (**12S-TS**). Although path Ib favours the formation of the *R*-configured product, path Ia *via* reaction channel **11**→**11S-TS**→**11S-prod** represents the lowest energy pathway alternative (Figure 8 and Figure 9).

As pointed out for **11S-TS** and **11R-TS** the oxidation process in **12S-TS** and **12R-TS** the geometry of the oxygen transfer is characterized by the closely linear arrangement of sulfur and peroxide oxygen atoms. Furthermore, the hydrogen bonding firmly keeps **1a** at the rear side of the TS structures in **12S-TS** and **12R-TS**.

The Inner Sphere Mechanism of the Sulfoxidation (Path II)

In previous studies^[2] mechanistic suggestions appeared for sulfoxidation of the imidazole sulfide-type precursors (such as **1a**) coordinated to titanium, therefore we have briefly explored this reaction path as well. As we shown above (see above), **1a** is readily coordinated to titanium, and thus complex **13** (Figure 10 and Figure 13) may also occur as reaction intermediate in the sulfoxidation reaction. However, the activation barrier (**13R-TS**) for the oxidation of the coordinated sulfide (Figure 10) is much higher (by 6–10 kcal mol⁻¹) than for the non-coordinated ones (such as for **11S-TS** and **11R-TS**, path Ia). The high activation barrier can be explained by dual geometrical constraints in the TS structure **13R-TS** (Figure 13). The oxidation process requires an O–O–S angle which is close to 180° and at the same time coordinative interactions between titanium and the imidazole nitrogen. This leads to a much more strained TS state geometry for the inner-sphere mechanism (path II) than for the out of sphere mechanistic path-

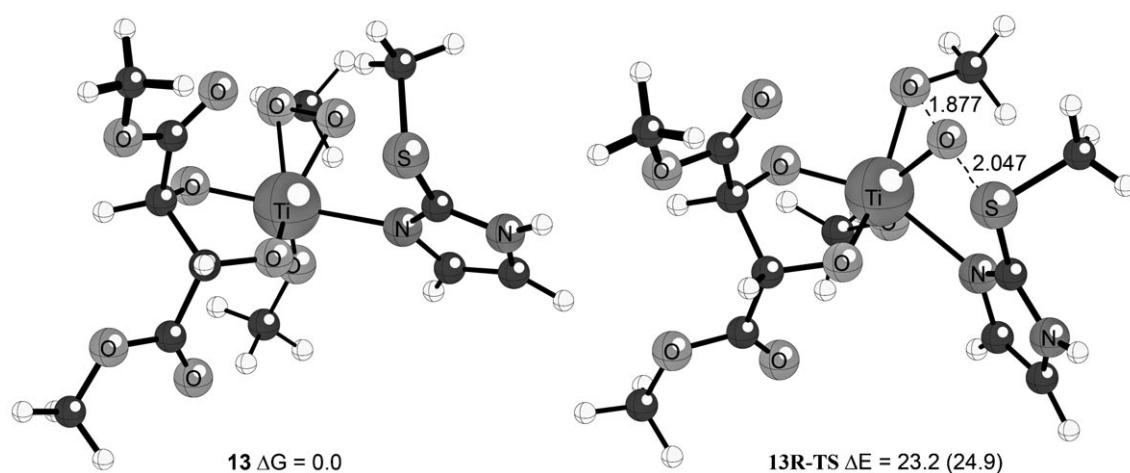


Figure 13. Selected calculated structures for path II (cf. Figure 11). The distances are given in Å units and the Gibbs free energy values and the total energy differences (in parentheses) are given in kcal mol⁻¹.

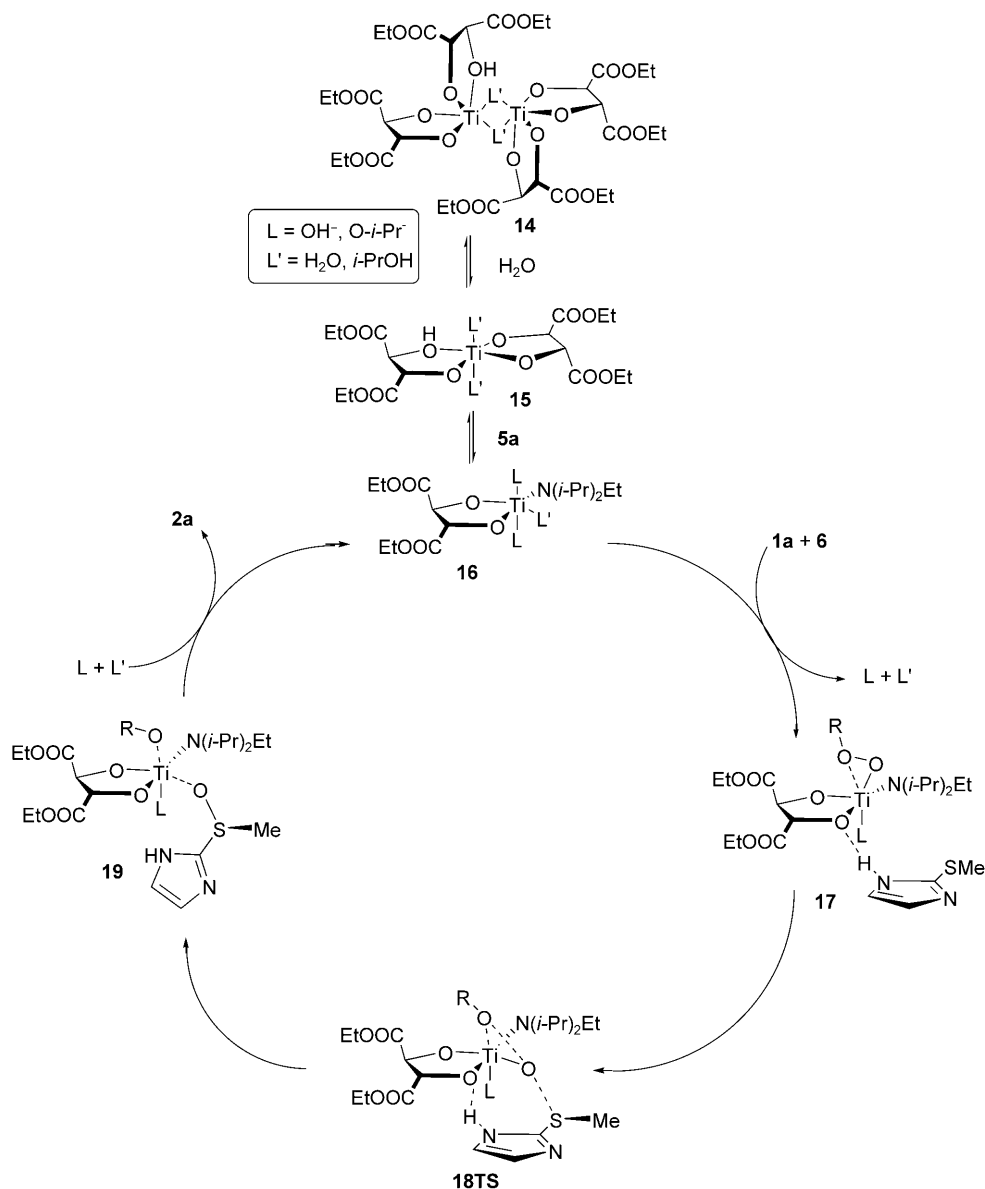


Figure 14. Mechanism of the asymmetric sulfoxidation of **1a** based on the above experimental and modelling results.

ways (paths Ia and Ib). Besides, in **13** and **13R-TS** the N–H group of imidazole is turned away from the tartrate ligand because of the coordination of the other nitrogen to titanium. Therefore, effective hydrogen bonding between the imidazole ring and the tartrate ligand is not possible. As this type of hydrogen bonding is essential for the asymmetric induction of the oxidation in **11S-TS**, the selective sulfoxidation is also difficult to explain for the inner sphere mechanism.

Mechanism of the Asymmetric Sulfoxidation

Based on the above results obtained from the APCI, NMR and DFT studies a catalytic cycle was constructed (Figure 14). The APCI studies (see above) indicate that added water facilitates the splitting of the binuclear complex **14** to a mononuclear analogue, such as **15**. According to the NMR studies (see above) the next step is coordination of the added amine (such as **5a**) to create the active intermediate (**16**) of the catalytic cycle. The peroxide reagent coordinates to titanium in an η^2 -fashion affording complex **17**. The DFT studies show that at least two different configurations (such as **11** and **12**) are possible for

complex **17** initiating two different reaction channels each (paths Ia and Ib). Starting from **17** the sulfoxidation reaction affords complex **19**. The enantioselectivity of the sulfoxidation is determined in this step of the catalytic cycle. We have localized a number of possible TS structures (**11R-TS**, **11S-TS**, **12R-TS**, **12S-TS** and **13R-TS**) for the enantioselectivity determining step of the process. According to the modelling studies the lowest energy path corresponds to the **11**→**11S-TS**→**11S-prod** process. Therefore, we propose that the lowest energy path in the sulfoxidation reaction proceeds *via* complex **18TS**, which is the realistic analogue of model structure **11S-TS**. In this complex the S-Me group points away the titanium atom inducing S-configuration on the sulfur in the oxidation process (see above).

As pointed out in the modelling studies, the chiral induction is governed by hydrogen bonding, interactions between the N–H group of the imidazole ring and the chiral tartrate ligand. Another important geometrical factor influencing the enantioselectivity is the stereoelectronic requirement^[60] of the sulfoxidation requiring a linear alignment of the peroxide oxygens and sulfur atom (O–O–S angle) in the TS structure. In complex **19** the oxygen of the sulfoxide group is coordinated to titanium. The final step of the process is decomplexation of the chiral sulfoxide product, such as **2a**, regenerating the catalyst.

Conclusions

The above studies have shown that the smallest subunit of pyrimetazole (**1h**) required for the high level of enantioselection in the esomeprazole process is an imidazole ring. Methyl imidazole sulfide **1a** could be oxidized as selectively as its functionalized analogues, such as **1c–e** and **1g–h**. However, nitrogen substitution of the imidazole ring leads to a major drop of the enantioselectivity. APCI studies indicate that addition of water to the reaction mixture of oxidation shifts the equilibrium toward formation of mononuclear titanium species providing the catalytically active species of the selective oxidation. According to our NMR studies the added amine is able to coordinate to titanium to create coordinatively saturated complexes. Thus, the prochiral sulfides are not coordinated to titanium but to the chiral tartrate ligand by hydrogen bonding. In the absence of an N–H group on the imidazole ring, such coordination is not possible, which is the probable explanation of the low enantioselectivity observed for oxidation of *N*-methyl analogues **1b** and **1f**. The stereoelectronic effects of the transfer of the oxygen atom from the peroxide reagent to the sulfur atom of the substrate impose an important geometrical constrain to the TS structure of the complex, by rendering the O–O–S angle to

closely linear. Because of this constraint inner sphere oxidation of the imidazole sulfides (path II) is unlikely, which is confirmed by the DFT modelling studies.

Assessment of the above mechanistic features affecting the level of enantioselection in the oxidation of prochiral nitrogen containing heterocyclic compounds, will hopefully inspire new laboratory as well as industrial processes for the preparation of chiral sulfoxides.

Experimental Section

Sulfides **1a–1g**^[12,69–71] and racemic sulfoxides^[12] (applied as standards for the determination of the *ee* values) were prepared according to the reported procedures. Unless otherwise stated the ¹H and ¹³C NMR spectra were recorded in CDCl₃ on Varian 300 or 400 MHz spectrometers. The chemical shifts (ppm) were obtained by using CHCl₃ as internal standard (¹H NMR: 7.26 ppm; ¹³C NMR: 77.36 ppm). The optical rotation data (*c*=g substance/100 mL solvent) were obtained on a Perkin–Elmer 241 polarimeter. The HPLC data was obtained on “Waters Acquity™ Ultraperformance LC” instrument (for chromatographic conditions see the corresponding entries).

General Procedure for Catalytic Oxidation of Sulfides

To a solution of sulfide **1** (0.25 mmol) in toluene (0.5 mL), water (0.001 mL, 0.055 mmol) and D-(–)-diethyl tartrate **4** (0.025 mL, 0.152 mmol) were added. This solution was heated to 50 °C and stirred at this temperature for 15 min. Then, titanium(IV) isopropoxide **3** (0.022 mL, 0.076 mmol) was added; and the reaction mixture was kept at 50 °C for 45 min. Subsequently, the temperature was lowered (see Table 1 for specific cases) followed by addition of diisopropylethylamine **5a** (0.013 mL, 0.076 mmol) and cumene hydroperoxide **6** (0.1 mL of 2.5 M solution in toluene, 0.25 mmol). The obtained reaction mixture was stirred for the allotted times and temperatures (Table 1). The reaction was then quenched by addition of water, followed by extraction with EtOAc (2 × 10 mL). The combined organic layers were washed with brine (1 × 5 mL), then dried (MgSO₄) and concentrated under vacuum. The crude product (**2**) was purified by column chromatography over silica gel using an appropriate ratio of pentane/EtOAc as eluent.

2-Methyl(sulfinyl)imidazole (2a): Sulfoxide **2a** was prepared according to the above general procedure, except that additional 1 mL of toluene was added to the reaction mixture after the addition of cumene hydroperoxide. The chiral sulfoxide **2a** was obtained as a white solid in 97% *ee*; yield: 62%. ¹H NMR: δ = 7.18 (s, 2H), 3.04 (s, 3H); ¹³C NMR: δ = 146.5, 125.7, 40.8; [α]_D²⁰: +73.3 (*c* 1.57, acetone). The *ee* was determined by HPLC (Chiralpak AS column, isohexane/*i*-PrOH, 90:10, flow rate 0.8 mL min^{–1}): *t*R (minor) = 29.8 min, *t*R (major) = 31.5 min, λ = 238.7 nm; HR-MS (ESI): *m/z* = 137.0358, calcd. for [C₄H₆N₂OS + Li]⁺: 137.0355. The absolute configuration of **2a** was determined by X-ray analysis.^[51]

2-Methyl(sulfinyl)-N-methylimidazole (2b): Sulfoxide **2b** was prepared according to the above general procedure,

except that the reaction was carried out in toluene- d_8 . The yield (33%) was determined by ^1H NMR spectroscopy using naphthalene as internal standard. The ^1H NMR shifts were determined from the crude reaction mixture. ^1H NMR (toluene- d_8): δ = 6.33 (d, J = 1.2 Hz, 1H), 6.26 (brs, 1H), 3.27 (s, 3H), 2.71 (s, 3H). Addition of shift reagent [(*S*)-(+)-*N*-(3,5-dinitrobenzoyl)- α -methylbenzylamine] showed that the product is racemic (<2% *ee*).

2-Benzyl(sulfinyl)imidazole (2c): Sulfoxide **2c** was prepared according to the above general procedure, except that additional 1 mL of toluene was added to the reaction mixture after the addition of cumene hydroperoxide. The chiral sulfoxide **2c** was obtained as a white solid in 95% *ee*; yield: 61%. ^1H NMR: δ = 11.59 (br s, 1H), 7.23 (m, 5H), 7.0 (m, 2H), 4.21 and 4.41 [d (AB-system), J = 13.5 Hz, 2H]; ^{13}C NMR: δ = 144.7, 130.7, 130.6, 129.1, 128.9, 128.8, 61.2; $[\alpha]_{\text{D}}^{20}$: -85.3 (c 1.04, acetone). The *ee* was determined by HPLC (Chiralcel OJ-H column, hexane/*i*-PrOH 80:20, flow rate 0.8 mL min $^{-1}$): *tR* (major) = 7.0 min; *tR* (minor) = 8.7 min, λ = 246.9 nm. HR-MS (ESI): m/z = 207.0584, calcd. for $[\text{C}_{10}\text{H}_{10}\text{N}_2\text{OS} + \text{H}]^+$: 207.0587.

4,5-Diphenyl-2-methyl(sulfinyl)imidazole (2d): Sulfoxide **2d** was prepared according to the above general procedure, except that additional 1 mL of toluene was added to the reaction mixture after the addition of cumene hydroperoxide. The chiral sulfoxide **2d** was obtained as a white solid in 80% *ee*; yield: 50%. ^1H NMR (DMSO- d_6): δ = 7.48 (d, J = 6.9 Hz, 4H), 7.35 (m, 6H), 3.09 (s, 3H); ^{13}C NMR (DMSO- d_6): δ = 148.4, 133.2, 129.2, 128.5, 39.5 (the quaternary carbons are not visible due to line broadening); $[\alpha]_{\text{D}}^{20}$: +37.6 (c 0.75, CHCl_3). The *ee* was determined by HPLC (Chiralpak AD-H column, hexane/*i*-PrOH, 95:5, flow rate 1.1 mL min $^{-1}$): *tR* (minor) = 8.5 min; *tR* (major) = 9.4 min, λ = 270.2 nm; HR-MS (ESI): m/z = 283.0897, calcd. for $[\text{C}_{16}\text{H}_{14}\text{N}_2\text{OS} + \text{H}]^+$: 283.0900.

2-Methyl(sulfinyl)benzimidazole (2e): This product was prepared according to the above general procedure affording **2e** as a white solid in 98% *ee*; yield: 65%. The ^1H NMR data obtained for **2e** agree with the literature values given for its racemic form.^[12] ^1H NMR: δ = 7.78, (br s, 1H), 7.58 (br s, 1H), 7.31 (m, 2H), 3.18 (s, 3H); ^{13}C NMR: δ = 153.9, 143.9, 134.9, 124.7, 123.5, 120.4, 112.5, 41.6; $[\alpha]_{\text{D}}^{20}$: +39.3 (c 5.53, acetone) Lit.^[72] $[\alpha]_{\text{D}}^{20}$: -20.8 (c 1.0, acetone) for (*R*), 61% *ee*. The *ee* was determined by HPLC (Chiralcel OJ-H column, isohexane/*i*-PrOH, 95:5, flow rate 0.8 mL min $^{-1}$): *tR* (major) = 20.9 min; *tR* (minor) = 26.5 min, λ = 280.2 nm; HR-MS (ESI): m/z = 181.0432, calcd. for $[\text{C}_8\text{H}_8\text{N}_2\text{OS} + \text{H}]^+$: 181.0430.

2-Methyl(sulfinyl)-*N*-methyl-benzimidazole (2f): This product was prepared according to the above general procedure affording **2f** as a white solid in <2% *ee*; yield: 48%. The ^1H NMR data obtained for **2f** agree with the literature values given for its racemic form.¹ ^1H NMR: δ = 7.82 (m, 1H), 7.42 (m, 2H), 7.36 (m, 1H), 4.14 (s, 3H), 3.26 (s, 3H); ^{13}C NMR: δ = 152.2, 141.9, 137.1, 124.8, 123.7, 121.2, 110.1, 39.3, 31.1; HR-MS (ESI): m/z = 195.0588, calcd. for $[\text{C}_9\text{H}_{10}\text{N}_2\text{OS} + \text{H}]^+$: 195.0587.

2-Methyl(sulfinyl)-5-methoxybenzimidazole (2g): Sulfoxide **2g** was prepared according to the above general procedure, except that additional 1 mL of toluene was added to the reaction mixture after the addition of cumene hydroperoxide. The chiral sulfoxide **2g** was obtained as a gummy gel

in 94% *ee*; yield: 63%. The ^1H NMR data obtained for **2g** agree with the literature values given for its racemic form.^[12] ^1H NMR (CD_3OD): δ = 7.50 (d, J = 8.59 Hz, 1H), 7.07 (s, 1H), 6.91 (dd, J = 2.49 Hz, 8.71 Hz, 1H), 3.78 (s, 3H), 3.08 (s, 3H); ^{13}C NMR (CD_3OD): δ = 159.9, 155.3, 140.2, 136.5, 119.4, 116.3, 99.1, 57.1, 41.9; $[\alpha]_{\text{D}}^{20}$: +45.7 (c 1.04, acetone). The *ee* was determined by HPLC (Chiralcel OJ-H column, hexane/*i*-PrOH, 90:10, flow rate 1.0 mL min $^{-1}$): *tR* (major) = 15.4 min; *tR* (minor) = 19.9 min, λ = 302.8 nm; HR-MS (ESI): m/z = 211.0539, calcd. for $[\text{C}_9\text{H}_{10}\text{N}_2\text{O}_2\text{S} + \text{H}]^+$: 211.0536.

Esomeprazole (2h): This product was prepared according to the above general procedure except that it was isolated as a potassium salt (78% yield and 97% *ee*) by addition of potassium methoxide to the reaction mixture. The ^1H NMR data obtained for **2h** agree with the literature values.^[2] ^1H NMR (DMSO- d_6): δ = 8.25 (s, 1H), 7.37 (d, J = 8.6 Hz, 1H), 7.02 (d, J = 2.6 Hz, 1H), 6.60 (dd, J = 2.5 Hz, 8.4 Hz, 1H), 4.72 and 4.46 [d (AB system), J = 12.7 Hz, 2H], 3.75 (s, 3H), 3.70 (s, 3H), 2.21 (s, 6H); ^{13}C NMR (DMSO- d_6): δ = 163.4, 161.8, 153.7, 151.9, 149.1, 147.0, 141.6, 126.5, 124.9, 117.5, 109.0, 99.4, 59.7, 55.2, 48.6, 12.9, 11.3; $[\alpha]_{\text{D}}^{20}$: +30.1 (c 1.0, H_2O); Lit.^[2] $[\alpha]_{\text{D}}^{20}$: +30.5 (c 1.0, H_2O) for (*S*), 99.5% *ee*. The *ee* was determined by HPLC (Chiralpak AD-H column, hexane/*i*-PrOH/AcOH, 50:50:0.1, flow rate 0.6 mL min $^{-1}$): *tR* (minor) = 9.9 min; *tR* (major) = 11.7 min, λ = 300.3 nm.

General Procedure for Preparation of the APCI/MS Sample

(a) Reaction mixture in the absence of added water: Diethyl tartrate **4** (0.013 mL, 0.076 mmol) and CHCl_3 (0.5 mL) were heated to 50°C for 15 min. Then, titanium(IV) isopropoxide **3** (0.011 mL, 0.038 mmol) was added; and the reaction mixture was kept at 50°C for 45 min. After cooling the reaction mixture to room temperature the solution was diluted with 5 mL of CHCl_3 . The turbid solution was centrifuged and the supernatant solution was used for analysis.

(b) Reaction mixture in the presence of added water: This sample was prepared according to the above general procedure except that the water (1 μL) was added.

Synthesis of Complexes 9 and 10

To a solution of **1a** (0.25 mmol) in CHCl_3 (0.5 mL), water (2.5 μL) and D-(−)-diethyl tartrate **4** (0.013 mL, 0.076 mmol) was added. This solution was heated to 50°C and stirred for 15 min. Then, titanium(IV) isopropoxide **3** (0.011 mL, 0.038 mmol) was added; and the reaction mixture was kept at 50°C for 45 min. Subsequently, the reaction mixture was cooled to room temperature and ether (6 mL) was added. The white precipitate (**9**) was separated by centrifugation. ^1H NMR (CD_3OD): δ = 7.34 (s, 2H), 4.55 (s, 2H), 4.26 (q, J = 7.08, 4H), 2.68 (s, 3H), 1.32 (t, J = 7.02, 6H); ^{13}C NMR (CD_3OD): δ = 171.53, 142.25, 122.07, 72.41, 61.14, 16.96, 13.06.

To complex **9** in CDCl_3 one equivalent of **5a** was added and the sample (**10**) was studied by ^{13}C NMR spectroscopy. ^{13}C NMR (CDCl_3) for **10**: δ = 171.90, 141.69, 72.39, 62.68, 51.79, 41.28, 19.75, 18.72, 16.81, 14.45.

Oxidation of **1a** with **9** as Catalyst

A chloroform solution (0.25 mL) of complex **9** (0.016 g, 0.038 mmol), **1a** (0.010 g, 0.087 mmol), **5a** (0.005 mL, 0.038 mmol) and water (1 μ L) was stirred for 1 h at 50 °C. Subsequently, the temperature was lowered to -20 °C followed by addition of cumene hydroperoxide **6** (0.05 mL of 2.5 M solution in CHCl₃, 0.125 mmol) and CHCl₃ (0.5 mL) and the obtained reaction mixture was stirred for 6 h. Then, the reaction was quenched with water, followed by addition of EtOAc (5 mL) and extraction with water (2 \times 5 mL). After evaporation the crude product (**2a**) was purified by column chromatography over silica gel using an appropriate ratio of pentane/EtOAc as eluent; yield: 45% yield, 79% ee). The ee was determined by HPLC (Chiralpak AS column, isohexane/*i*-PrOH, 90:10, flow rate 0.8 mL min⁻¹): tR (minor) = 29.8 min; tR (major) = 31.5 min, λ = 238.7 nm.

Supporting Information

Cartesian coordinates for species **11–13**, NMR spectra for **2a–i** and complex **9** and simulations of the isotope patterns of complexes **7** and **8** are available as Supporting Information.

Acknowledgements

This work was supported by the Swedish Natural Science Research Council (VR) and Global Process R&D AstraZeneca. The support and discussions with Dr. Magnus Larsson (Process R&D Södertälje, AstraZeneca, Sweden) are gratefully acknowledged. The authors are also indebted to the Alice and Knut Wallenberg Foundation for funding a UPLC instrument.

References

- [1] H.-J. Federsel, M. Larsson, in: *Asymmetric Catalysis on Industrial Scale*, (Eds.: H.-U. Blaser, E. Schmidt), Wiley-VCH, Weinheim, **2004**, p 413.
- [2] H. Cotton, T. Elebring, M. Larsson, L. Li, H. Sörensen, S. v. Unge, *Tetrahedron: Asymmetry* **2000**, *11*, 3819.
- [3] H.-J. Federsel, *Nat. Rev. Drug Discovery* **2005**, *4*, 685.
- [4] H.-J. Federsel, *Drug Discovery Today* **2006**, *11*, 966.
- [5] H. B. Kagan, T. O. Luukas, *Catalytic Asymmetric Sulfide Oxidations*, Vol. 2, Wiley, Weinheim, **2004**.
- [6] H. B. Kagan, *Asymmetric Oxidation of Sulfides*, Wiley, Weinheim, **2000**.
- [7] J. Legros, J. R. Dehli, C. Bolm, *Adv. Synth. Catal.* **2005**, *347*, 19.
- [8] C. Bolm, K. Muñoz, J. P. Hildebrand, in: *Comprehensive Asymmetric Catalysis*, Vol. II, (Eds.: E. N. Jacobsen, A. Pfaltz, H. Yamamoto), Springer, Berlin, **1999**, p 697.
- [9] I. Fernández, N. Khiar, *Chem. Rev.* **2003**, *103*, 3651.
- [10] K. P. Bryliakov, E. P. Talsi, *Curr. Org. Chem.* **2008**, *12*, 386.
- [11] M. C. Carreño, *Chem. Rev.* **1995**, *95*, 1717.
- [12] J. M. Shin, Y. M. Cho, G. Sachs, *J. Am. Chem. Soc.* **2004**, *126*, 7800.
- [13] D. M. Tavish, M. M. Buckley, R. C. Heel, *Drugs* **1991**, *42*, 138.
- [14] S. Okabe, K. Shimosako, K. Amagase, *J. Physiol. Pharmacol.* **2001**, *52*, 639.
- [15] C. M. Spencer, D. Faulds, *Drugs* **2000**, *60*, 321.
- [16] M. Salas, A. Ward, J. Caro, *BMC Gastroenterology* **2002**, *2*, 17.
- [17] C. Perez-Giraldo, G. Cruz-Villalon, R. Sanchez-Silos, R. Martinez-Rubio, M. T. Blanco, A. C. Comez-Garcia, *J. Appl. Microbiol.* **2003**, *95*, 709.
- [18] K. C. Agarwal, *Med. Res. Rev.* **1996**, *16*, 111.
- [19] M. A. Adetumjibi, B. H. Lau, *Med. Hypotheses* **1983**, *12*, 227.
- [20] G. Merino, A. J. Molina, J. L. Garcia, M. M. Pulido, J. G. Prieto, A. I. Alvarez, *Pharm. Pharmacol.* **2003**, *55*, 757.
- [21] R. Schmied, G. X. Wang, M. Korth, *Circ. Res.* **1991**, *68*, 597.
- [22] A. V. Nieves, A. E. Lang, *Clin. Neuropharmacol.* **2002**, *25*, 111.
- [23] S. Padmanabhan, R. C. Lavin, G. J. Gurant, *Tetrahedron: Asymmetry* **2000**, *11*, 3455.
- [24] P. Pitchen, E. Duñach, M. N. Deshmukh, H. B. Kagan, *J. Am. Chem. Soc.* **1984**, *106*, 8188.
- [25] J.-M. Brunel, P. Diter, M. Duetsch, H. B. Kagan, *J. Org. Chem.* **1995**, *60*, 8086.
- [26] S. H. Zhao, O. Samuel, H. B. Kagan, *Tetrahedron* **1987**, *43*, 5135.
- [27] N. Komatsu, M. Haahizume, T. Sugita, S. Uemura, *J. Org. Chem.* **1993**, *58*, 4529.
- [28] N. Komatsu, M. Haahizume, T. Sugita, S. Uemura, *J. Org. Chem.* **1993**, *58*, 7624.
- [29] M. T. Reetz, C. Merk, G. Naberfeld, J. Rudolph, N. Griebenow, R. Goddard, *Tetrahedron Lett.* **1997**, *38*, 5273.
- [30] C. Bolm, O. A. G. Dabard, *Synlett* **1999**, 360.
- [31] F. D. Furia, G. Licini, G. Modena, R. Motterle, W. A. Nugent, *J. Org. Chem.* **1996**, *61*, 5175.
- [32] M. Bonchio, S. Calloni, F. D. Furia, G. Lichini, G. Modena, S. Moro, W. A. Nugent, *J. Am. Chem. Soc.* **1997**, *119*, 6935.
- [33] G. Licini, M. Bonchio, G. Modena, W. A. Nugent, *Pure Appl. Chem.* **1999**, *71*, 463.
- [34] K. P. Bryliakov, E. P. Talsi, *Eur. J. Org. Chem.* **2008**, 3369.
- [35] A. Thompson, J. R. Garabatos-Perera, H. M. Gillis, *Can. J. Chem.* **2008**, *86*, 676.
- [36] A. Lattanzi, S. Piccirillo, A. Scettri, *Adv. Synth. Catal.* **2007**, *349*, 357.
- [37] M. Palucki, P. Hanson, E. N. Jacobsen, *Tetrahedron Lett.* **1992**, *33*, 7111.
- [38] C. Kokubo, T. Katsuki, *Tetrahedron* **1996**, *52*, 13895.
- [39] K. Noda, N. Hosoya, K. Yanai, T. Katsuki, *Tetrahedron Lett.* **1994**, *35*, 1887.
- [40] C. Bolm, F. Bienewald, *Angew. Chem.* **1995**, *107*, 2883; *Angew. Chem. Int. Ed. Engl.* **1995**, *34*, 2640.
- [41] C. Bolm, F. Bienewald, *Synlett* **1998**, *34*, 1327.
- [42] S. A. Blum, R. G. Bergman, J. A. Ellman, *J. Org. Chem.* **2003**, *68*, 150.
- [43] D. J. Weix, J. A. Ellman, *Org. Lett.* **2003**, *5*, 1317.
- [44] K. Nakajima, M. Kojima, J. Fujita, *Chem. Lett.* **1986**, 1483.

- [45] A. Pordea, M. Creus, J. Panek, C. Duboc, D. Mathis, M. Novic, T. R. Ward, *J. Am. Chem. Soc.* **2008**, *130*, 8055.
- [46] P. Kelly, S. E. Lawrence, A. R. Maguire, *Synlett* **2006**, 1569.
- [47] J. Legros, C. Bolm, *Angew. Chem.* **2003**, *115*, 5636; *Angew. Chem. Int. Ed.* **2003**, *42*, 5478.
- [48] J. Legros, C. Bolm, *Angew. Chem.* **2004**, *116*, 4321; *Angew. Chem. Int. Ed.* **2004**, *43*, 4225.
- [49] J. Legros, C. Bolm, *Chem. Eur. J.* **2005**, *11*, 1086.
- [50] K. Matsumoto, T. Yamaguchi, T. Katsuki, *Chem. Commun.* **2008**, 1704.
- [51] M. Seenivasaperumal, H.-J. Federsel, A. Ertan, K. J. Szabó, *Chem. Commun.* **2007**, 2187.
- [52] T. Katsuki, K. B. Sharpless, *J. Am. Chem. Soc.* **1980**, *102*, 5976.
- [53] I. D. Williams, S. F. Pedersen, K. B. Sharpless, S. J. Lipard, *J. Am. Chem. Soc.* **1984**, *106*, 6430.
- [54] S. F. Pedersen, J. C. Dewan, R. R. Eckman, K. B. Sharpless, *J. Am. Chem. Soc.* **1987**, *109*, 1279.
- [55] M. Herderich, E. Richling, R. Roscher, C. Schneider, W. Schwab, H.-U. Humpf, P. Schreier, *Chromatographia* **1997**, *45*, 127.
- [56] W. M. A. Nilssen, A. P. Tinke, *J. Chromatogr. A* **1995**, *703*, 37.
- [57] W. J. Evans, K. A. Miller, J. W. Ziller, J. Greaves, *Inorg. Chem.* **2007**, *46*, 8008.
- [58] M. E. Rybak, D. L. Parker, C. M. Pfeiffer, *J. Chromatogr. B* **2008**, *861*, 145.
- [59] P. Zöllner, B. Hayer-Helm, *J. Chromatogr. A* **2006**, *1136*, 123.
- [60] K. A. Jørgensen, *J. Chem. Soc. Perkin Trans. 2* **1994**, 117.
- [61] A. D. Becke, *J. Chem. Phys.* **1993**, *98*, 5648.
- [62] C. Lee, W. Yang, R. G. Parr, *Phys. Rev.* **1988**, *B 37*, 785.
- [63] B. Miehlich, A. Savin, H. Stoll, H. Preuss, *Chem. Phys. Lett.* **1989**, *157*, 200.
- [64] P. C. Hariharan, J. A. Pople, *Mol. Phys.* **1974**, *27*, 209.
- [65] V. A. Rasslov, J. A. Pople, M. A. Ratner, T. L. Windus, *J. Chem. Phys.* **1998**, *109*, 1223.
- [66] M. J. Frisch, G. W. Trucks, H. B. Schlegel, G. E. Scuseria, M. A. Robb, J. R. Cheeseman, J. A. Montgomery, T. Vreven, K. N. Kudin, J. C. Burant, J. M. Millam, S. S. Iyengar, J. Tomasi, V. Barone, B. Mennucci, M. Cossi, G. Scalmani, N. Rega, G. A. Petersson, H. Nakatsuji, M. Hada, M. Ehara, K. Toyota, R. Fukuda, J. Hasegawa, M. Ishida, T. Nakajima, Y. Honda, O. Kitao, H. Nakai, M. Klene, X. Li, J. E. Knox, H. P. Hratchian, J. B. Cross, C. Adamo, J. Jaramillo, R. Gomperts, R. E. Stratmann, O. Yazyev, A. J. Austin, R. Cammi, C. Pomelli, J. W. Ochterski, P. Y. Ayala, K. Morokuma, G. A. Voth, P. Salvador, J. J. Dannenberg, V. G. Zakrzewski, S. Dapprich, A. D. Daniels, M. C. Strain, O. Farkas, D. K. Malick, A. D. Rabuck, K. Raghavachari, J. B. Foresman, J. V. Ortiz, Q. Cui, A. G. Baboul, S. Clifford, J. Cioslowski, B. B. Stefanov, G. Liu, A. Liashenko, P. Piskorz, I. Komaromi, R. L. Martin, D. J. Fox, T. Keith, M. A. Al-Laham, C. Y. Peng, A. Nanayakkara, M. Challacombe, P. M. W. Gill, B. Johnson, W. Chen, M. W. Wong, C. Gonzalez, J. A. Pople, *Gaussian 03*, Gaussian, Inc., Wallingford CT, **2003**.
- [67] G. Boche, K. Möbus, K. Harms, M. Marsch, *J. Am. Chem. Soc.* **1996**, *118*, 2770.
- [68] K. A. Jørgensen, R. A. Wheeler, R. Hoffmann, *J. Am. Chem. Soc.* **1987**, *109*, 3240.
- [69] M. S. C. Pedras, A. Q. Khan, *J. Agric. Food Chem.* **1996**, *44*, 3403.
- [70] M. S. C. Pedras, M. Jha, *J. Org. Chem.* **2005**, *70*, 1828.
- [71] B. R. Rani, U. T. Bhalero, M. F. Rahman, *Synth. Commun.* **1990**, *20*, 3045.
- [72] E. Duñach, H. B. Kagan, *Nouv. J. Chimie* **1985**, *9*, 1.